Influence of the Bridging Azine Ligand on the Rate of Ligand Substitution in a Series of Dinuclear Platinum(II) Complexes

D. REDDY, D. JAGANYI

School of Chemistry, University of KwaZulu-Natal, Private Bag X01, Scottsville, Pietermaritzburg, 3209, South Africa

Received 20 December 2009; revised 9 July 2010, 23 August 2010; accepted 23 August 2010

DOI 10.1002/kin.20529
Published online 16 February 2011 in Wiley Online Library (wileyonlinelibrary.com).

ABSTRACT: A series of azine-bridged dinuclear platinum(II) complexes of the type $[\{trans\text{-}Pt(NH_3)_2(OH_2)\}_2(\mu\text{-azn})](ClO_4)_4$ (where azn = pyrazine (pzn, **Pt1**), 2,3-dimethylpyrazine (2,3-pzn, **Pt2**), and 2,5-dimethylpyrazine (2,5-pzn, **Pt3**)) were synthesized to investigate the influence of the bridging azine ligand on the reactivity of the platinum(II) centers. The pK_a values of the complexes were determined via acid–base titration, and the rate of substitution of the aqua moiety by a series of neutral nucleophiles, viz. thiourea (TU), 1,3-dimethyl-2-thiourea (DMTU), and 1,1,3,3-tetramethyl-2-thiourea (TMTU), was determined under pseudo-first-order conditions as a function of concentration and temperature using standard spectrophotometric techniques. The introduction of the methyl groups to the bridging azine linker in **Pt2** and **Pt3** leads to a moderate increase in the pK_a values obtained for the first and second deprotonation steps, respectively, as a result of the increased σ-donor capacity of the bridging azine ligand trans to the aqua moiety. A comparison of the rate constants, k_1 and k_2, at 298 K, obtained for the substitution of the aqua moieties from **Pt1**, **Pt2**, and **Pt3** by TU, shows that the introduction of the σ-donating methyl groups on the bridging azine ligand in **Pt2** and **Pt3** results in a corresponding decrease in the reactivity, by ca. five times for the first substitution step and ca. 10 times for the second substitution step. Density functional theory calculations at the B3LYP/LACVP** level of theory for the complexes demonstrate that the introduction of electron-donating methyl groups results in (i) increased steric hindrance over the metal centers and (ii) decreased the positive charge on the metal center and increases energy separation of the frontier molecular orbitals ($E_{HOMO} - E_{LUMO}$) of the ground-state platinum(II) complexes, leading to a less-reactive metal center. © 2011 Wiley Periodicals, Inc. Int J Chem Kinet 43: 161–174, 2011

Correspondence to: D. Jaganyi; e-mail: jaganyi@ukzn.ac.za.
Contract grant sponsor: University of KwaZulu-Natal.
Contract grant sponsor: South African National Research Foundation (NRF).
Supporting Information is available in the online issue at www.wileyonlinelibrary.com.

INTRODUCTION

The use of platinum coordination compounds in cancer chemotherapy has been extensively studied following the fortuitous discovery of the therapeutic properties of *cis*-diamminedichloroplatinum(II) (*cis*-$[Pt(NH_3)_2Cl_2]$, cisplatin) by Rosenberg et al. [1,2]. First approved for the treatment of testicular cancer in 1978, cisplatin is one of the most widely utilized antitumor drugs, exhibiting high efficacy against solid tumors, particularly testicular and ovarian cancer [3–8]. Despite the remarkable success of cisplatin, several problems have been found in clinical use. First, cisplatin treatment is often accompanied by severe side effects, including cumulative toxicities of nephrotoxicity, neurotoxicity, and emetogenesis [5,6,9–11]. In addition, cisplatin activity is limited to a relatively narrow range of tumors as a result of inherent or treatment-induced tumor resistance [6,12].

As a result of these drawbacks, research in recent years has focused on nonclassical platinum complexes, i.e., those that do not obey the structure–activity rules first established for platinum chemotherapy drugs based on the results obtained for cisplatin [13,14]. Among these is the antitumor activity of multinuclear platinum complexes, typically consisting of either two or three platinum centers that are linked through a bridging ligand [15–25]. The success of these systems is based on the ability of these complexes to form DNA adducts that are structurally different from those formed by cisplatin and its related analogues [26,27].

The major product of cisplatin interaction with genomic DNA is a 1,2-intrastrand cross-link, which induces a kink on the DNA double helix [28,29]. These conformational changes are believed to play an important role in the development of cisplatin resistance [30]. Therefore, compounds capable of binding to DNA in a significantly different manner should, theoretically, overcome the problem of resistance.

Another apparent advantage of these multinuclear (mostly dinuclear) complexes is the high charge (+4), as compared to the neutral mononuclear complexes, which offers better solubility, more efficient electrostatic interaction with the polyanionic DNA, and faster uptake [31].

These multinuclear antitumor active platinum(II) complexes typically comprise one of two types of bridging ligands, viz. flexible [15–17,32], e.g., aliphatic diamines, or rigid [18,19,22,33–35], e.g., azoles and azines. Those with flexible linkers are more suited to forming long-range cross-links on DNA [36,37], whereas those with rigid linkers are designed such that they minimize distortion of the DNA double helix in a 1,2-intrastrand cross-link [33].

Thus, it can be seen that comprehensive studies on the role of the DNA-binding properties and product formation have been conducted on these dinuclear platinum(II) complexes, with results being interpreted in terms of charge, hydrogen bonding, length, and flexibility of the bridging ligand. However, there is limited information in the literature with regard to the reactivity and thermodynamic properties of the two platinum centers in these types of complexes [38–43]. Some data [38,39] suggest that the reactivity and properties of the first platinum center are independent of the state of the second and vice versa. van Eldik et al. [42–45] have demonstrated that there is a clear interaction between the two platinum(II) centers that becomes weaker as the length of the aliphatic chain linker is increased.

It is therefore the aim of this paper to highlight the effect of the rigid bridging azine ligand on the reactivity of the metal center.

MATERIALS AND METHODS

Reactions used in the synthesis of the platinum(II) complexes were all carried out in air unless otherwise stated. *trans*-Diamminedichlororplatinum(II) (*trans*-$[Pt(NH_3)_2Cl_2]$, 99.99%), pyrazine (pzn, $\geq$ 99%), 2,3-dimethylpyrazine (2,3-pzn, 99%), 2,5-dimethylpyrazine (2,5-pzn, 98%), and sodium perchlorate monohydrate* ($NaClO_4 \cdot H_2O$, 98%) were purchased from Aldrich (Capital Lab Supplies CC, New Germany, South Africa) and used without further purification. Silver perchlorate* ($AgClO_4$, 99.998%, Aldrich) was stored under nitrogen and used as supplied. Perchloric acid ($HClO_4$, 70% solution), *N*,*N*-dimethylformamide (DMF, 99.0%), and sodium hydroxide (NaOH) was obtained from Saarchem (Merck Chemicals, Wadeville, South Africa) and used as supplied. Buffer solutions of pH 4, 7, and 10 were purchased from Saarchem.

The nucleophiles, thiourea (TU, 99%), 1,3-dimethyl-2-thiourea (DMTU, 99%), and 1,1,3,3-tetramethyl-2-thiourea (TMTU, 98%)† were obtained from Aldrich and used without further purification. Ultrapure water (Modulab Systems, Continental Water

*Perchlorate salts are known to be explosive oxidizers, and their use warrants extra caution. Sodium perchlorate in particular is a known irritant and targets human tissue and organs, viz. the thyroid and blood.

†Thiourea and its substituted derivatives are suspected carcinogens and the necessary safety precautions must be adhered to when handling these reagents.

Systems, NSW, Australia) was used for all aqueous reactions. All other chemicals were of analytical reagent quality.

The platinum(II) precursor, *trans*-[$PtCl(NH_3)_2DMF](ClO_4$) (**1**) [33,46,47], the azine-bridged dinuclear platinum(II) chloro complexes, viz. [{*trans*-$PtCl(NH_3)_2$}$_2$(μ-pzn)]$(ClO_4)_2$ (**Pt1-Chloro**), [{*trans*-$PtCl(NH_3)_2$}$_2$(μ-2,3-pzn)]$(ClO_4)_2$ (**Pt2-Chloro**), and [{*trans*-$PtCl(NH_3)_2$}$_2$(μ-2,5-pzn)]$(ClO_4)_2$ (**Pt3-Chloro**) [33,34] were synthesized by adaptations of established literature procedures. The azine-bridged dinuclear platinum(II) chloro complexes were converted into their corresponding aqua complexes using the method of Bugarćić et al. [48].

Synthesis of the Platinum(II) Complexes

trans-[PtCl(NH$_3$)$_2$DMF](ClO$_4$) (1). To a stirred suspension of *trans*-diamminedichloroplatinum(II) (0.600 g, 1.99 mmol) in DMF (35 mL) at 30°C in the dark, a solution of $AgClO_4$ (0.403 g, 1.94 mmol, 0.97 eq.) in DMF (15 mL) was added dropwise over 3 h. The resulting solution was stirred at 30°C in the dark for a period of 18 h. Thereafter, the yellow solution was allowed to cool and subsequently filtered through a 0.45-μm nylon membrane filter to remove the precipitated AgCl. The reaction flask and precipitate were rinsed with a small amount of cold DMF. The washings and filtrate were then transferred to a 100-mL volumetric flask and made up to the mark with DMF to afford a yellow solution of *trans*-[$PtCl(NH_3)_2DMF](ClO_4$) of the concentration 19.4 mM.

[{trans-PtCl(NH$_3$)$_2$}$_2$-μ-azn](ClO$_4$)$_2$ (Pt(1, 2 or 3)-Chloro). To a stirred solution of *trans*-[$PtCl(NH_3)_2DMF](ClO_4$) (**1**) (25 mL, 0.486 mmol) at 30°C, a solution of the respective azine linker (0.233 mmol, 0.48 eq.) in DMF (15 mL) was added. The resulting pale-yellow solution was stirred for an amount of time, dependent upon the linker used, i.e., pzn 2 h, 2,5-pzn 6 h, and 2,3-pzn 12 h. The solution was thereafter concentrated on a rotary evaporator. The residue was collected by filtration and rinsed with copious amounts of diethyl ether. The crude product was redissolved in a minimal amount of warm water and filtered through a 0.45-μm nylon membrane filter. The filtrate was evaporated to dryness. The pale-yellow product was rinsed with a small amount of diethyl ether and dried in a desiccator over P_2O_5.

[{trans-PtCl(NH$_3$)$_2$}$_2$-μ-pzn](ClO$_4$)$_2$ (Pt1-Chloro). Yield: 0.085 g (45%). Anal. Calcd for $Pt_2Cl_4O_8C_4H_{16}N_6$: C, 5.94; H, 2.00; N, 10.40. Found: C, 5.84; H, 2.06; N, 10.44. IR‡ (KBr) cm^{-1} = 344 (m), 484 (w), 532 (w), 625 (s), 820 (m), 933 (w), 1085 (vs), 1101 (vs), 1162 (sh), 1330 (m), 1436 (m), 1618 (b), 2015 (w), 3053 (m), 3241 (m), 3309 (s), 3405 (sh).

[{trans-PtCl(NH$_3$)$_2$}$_2$-μ-2,3pzn](ClO$_4$)$_2$(Pt2-Chloro). Yield: 0.073 g (37%). Anal. Calcd for $Pt_2Cl_4O_8C_6H_{20}N_6$: C, 8.62; H, 2.41; N, 10.05. Found: C, 8.61; H, 2.51; N, 9.99. IR† (KBr) cm^{-1} = 346 (m), 461 (w), 560 (w), 625 (s), 823 (sh), 834 (m), 933 (w), 985 (sh), 1016 (w, sh), 1092 (vs), 1198 (m), 1258 (w), 1324 (s), 1341 (s), 1415 (m), 1439 (m), 1618 (b), 2015 (w), 3101 (m), 3227 (m), 3305 (s), 3417 (sh).

[{trans-PtCl(NH$_3$)$_2$}$_2$-μ-2,5pzn](ClO$_4$)$_2$(Pt3-Chloro). Yield: 0.081g (41%). Anal. Calcd for $Pt_2Cl_4O_8C_6H_{20}N_6$: C, 8.62; H, 2.41; N, 10.05. Found: C, 8.18; H, 2.45; N, 10.21. IR‡ (KBr) cm^{-1}: 345 (m), 451 (w), 623 (s), 828 (sh), 884 (m), 932 (w), 1091 (vs), 1164 (m), 1288 (sh), 1333 (s), 1386 (w), 1504 (m), 1625 (b), 2017 (w), 3059(w), 3237 (m), 3309 (s).

Computational Modeling

Preliminary modeling of the complexes was performed using the computational software package, Spartan '04 for Windows [49,50], using the B3LYP [51] density functional method (DFT) [52,53] and the LACVP+** (Los Alamos Core Valence Potentials) [54] pseudopotential basis set. B3LYP relates to the hybrid functional Becke's three-parameter formulation [51], which has been proven to be superior to traditional functionals. The LACVP basis set employs effective core potentials for K–Cu, Pb–Ag, Cs–La, and Hf–Au, whereas Pople's 6-31G** basis set describes second- and third-row s- and p-block elements [55,56].

pK_a Determination of the Platinum(II) Dinuclear Complexes

Preparation of Complex Solutions for pK_a Determination. The aqua complexes (**Pt1**, **Pt2**, and **Pt3**) were prepared according to the method of Bugarćić et al. [48]. A known amount of the chloro complex was reacted with 1.96 molar equiv of silver perchlorate, $AgClO_4$, in 0.1 M $HClO_4$. The perchlorate ion, ClO_4^-, is not known to coordinate Pt(II) [57], and hence the substitution reactions of the platinum complexes with the given nucleophiles are unaffected by the presence

‡Designation: w = weak, m = medium, s = strong, vs = very strong, sh = shoulder, b = broad.

of this ion. The solution was then stirred at ca. 50°C for 24 h in the dark, after which the white precipitate of silver chloride that formed was separated from the mixture by filtration through a 0.45-μm nylon membrane filter using a Millipore filtration apparatus. The clear, colorless filtrate was then made to the required concentration in a volumetric flask using a solution of 0.1 M $HClO_4$. The use of the acidic solution ($HClO_4$, 0.1 M, pH 1) was necessary to ensure that only the aqua complex, and not a mixture of the aqua and hydroxo complexes, was present in solution once the metathesis reaction was complete, and also, to ensure a constant ionic strength of 0.1 M.

pK*$_a$ *Determination. UV–vis spectra for the determination of the pK_a values were recorded on a Varian Cary 100 Bio spectrophotometer. The pH of the solutions was recorded using a Jenway 4330 conductivity/pH meter fitted with a Micro 4.5-mm diameter glass electrode. Calibration of the electrode was achieved through the use of buffers of pH 4, 7, and 10 at 25°C. To avoid precipitation of $KClO_4$ within the electrode, the KCl solution was replaced with a 3 M NaCl solution.

Preparation of the aqua complexes is as described earlier. The starting concentration of the complexes was 0.16, 0.13, and 0.13 mM for the aqua analogues of complexes **Pt1**, **2**, and **3**, respectively. Spectrophotometric pH titrations of the aqua complex solutions, from pH 1 to 10 were performed using NaOH as the base. A large volume (100 mL) of the complex solution was used so as to avoid absorbance changes due to dilution effects. Initially, crushed pellets of NaOH were used to obtain a pH change from 1 to 3. All subsequent pH measurements were obtained by dipping a needle into a saturated solution of NaOH and thereafter into the complex solution. It was found that if the pH electrode was dipped into the test solution for a long period of time, it resulted in the formation of the chloro complex. It was therefore necessary to take 0.6-mL aliquots from the complex solution, which was then transferred into narrow vials for the pH measurements. These were then discarded after each measurement.

The reversibility of the titration was also tested using aqueous solutions of perchloric acid. The pK_a values were thereafter determined using the method described by van Eldik et al. [42,44].

Instrumentation and Physical Measurements

Elemental analyses were performed at the Institute for Inorganic Chemistry, University of Erlangen-Nürnberg, Erlangen, Germany. Infrared spectra were recorded, unless otherwise stated, using KBr disks on a Perkin Elmer Spectrum One FTIR spectrometer. UV/visible absorption spectra were recorded using a Varian Cary 100 Bio spectrophotometer.

All kinetic measurements were performed under pseudo-first-order conditions using, initially, UV/visible absorption spectra to determine the suitable wavelength at which kinetic investigations could be performed; these were recorded using a Varian Cary 100 Bio, and subsequently either the Varian Cary 100 Bio spectrophotometer with an online kinetic utility or an Applied Photophysics SX.18MV (v4.33) stopped-flow system coupled to an online data acquisition system, was used to monitor the kinetic process. All measurements were performed in a thermostated environment to within ±0.1°C. All data were graphically analyzed using the software package Origin 7.5 [58].

Preparation of Complex and Nucleophile Solutions for Kinetic Analysis. The preparation of the solutions of the aqua complexes and the respective nucleophiles for kinetic analysis was performed in a manner slightly different to that described for that during pK_a. The aqueous solvent system chosen was prepared such that it was pH 2 (0.01 M) $HClO_4$ and 0.09 M $NaClO_4$ while still maintaining a constant ionic strength (I) of 0.1 M ClO_4^-.

A known amount of the chloro complex was reacted with 1.96 molar equivalents of silver perchlorate, $AgClO_4$, in the solvent system described above. The solution was then stirred at ca. 50°C for 24 h in the dark, after which the white precipitate of silver chloride that formed was separated from the mixture by filtration through a 0.45-μm nylon membrane filter using a Millipore filtration apparatus. The clear, colorless filtrate was then made to the required concentration in a volumetric flask using the I = 0.1 M ClO_4^- solution. The use of the acidified solvent system ($HClO_4$ pH = 2) was necessary to ensure that only the aqua complex, and not a mixture of the aqua and hydroxo complexes, was present in solution once the metathesis reaction was complete.

Solutions of the neutral nucleophiles, viz. TU, DMTU, and TMTU, were prepared by dissolving a known amount of the required nucleophile in 100 mL of a solution having fixed ionic strength (i.e., the 0.1 M ClO_4^- solution containing 0.01 M $HClO_4$ and 0.09 M $NaClO_4$) to afford a final concentration that was ca. 100 times greater than that of the metal complex, while maintaining an ionic strength of 0.1 M. Subsequent dilutions with the same solution of fixed ionic

strength afforded a series of concentrations, in the order of 20, 40, 60, 80, and 100 times the concentration of the metal complex. These concentrations were chosen so as to maintain pseudo-first-order conditions, and the concentration of the nucleophile was in at least 10-fold excess with respect to each of the platinum-bound aqua moieties.

Kinetic Analyses. With the exception of **Pt1** + TU (or DMTU) all subsequent ligand substitutions reached completion after 16 min, viz. **Pt1** + TMTU, **Pt2** (or **Pt3**) + Nu (where Nu = TU, DMTU, and TMTU) and were spectrophotometrically monitored using a Cary 100 Bio UV/visible spectrophotometer, equipped with a Varian Peltier temperature controller and coupled to an online kinetics application. The substitutions were followed on the timescale that had been established during preliminary investigations and substitution reactions which reached completion before 16 min had elapsed, viz. **Pt1** + TU (or DMTU) were monitored using a thermostated stopped-flow apparatus. These substitution reactions were each followed for at least eight half-lives.

All kinetic measurements were best described by a double exponential equation. The observed pseudo-first-order rate constants, k_{obs1} and k_{obs2}, were calculated using the online nonlinear least-squares fit of exponential data.

The dependence of the rate constant on the incoming nucleophile concentration was analyzed in this manner for all nucleophiles while maintaining the temperature at 25°C. The second-order rate constants, k_1 and k_2, for the reaction of each metal complex with a particular nucleophile was obtained from the slope of a linear regression of a plot of the observed rate constants, k_{obs1} and k_{obs2}, versus the nucleophile concentration using Origin 7.5 [58]. For each of the nucleophiles, no meaningful intercepts were found and thus all plots can be described by Eq. (1) [59]

$$k_{obs(1,2)} = k(1, 2)[\mathrm{Nu}] \tag{1}$$

The dependence of the rate constant on temperature was conducted in a similar manner, with the nucleophile concentration being held constant at 30 times the concentration of the metal complex while varying the temperature from 15°C to 35°C at 5°C intervals. The values of the observed rate constants, k_{obs}, were converted to the respective k_1 and k_2 values (assuming a zero intercept), and these were applied to the Eyring equation to determine the activation parameters, $\Delta H^{\neq}$ and $\Delta S^{\neq}$ [59].

RESULTS

A series of three azine-bridged dinuclear platinum(II) complexes of the type $[\{trans\text{-}Pt(NH_3)_2(OH_2)\}_2(\mu\text{-azn})](ClO_4)_4$ (Scheme 1) were synthesized via adaptations of established literature procedures [33,34] in an effort to determine the influence of the bridging azine ligand on the rate of substitution of the aqua moiety from the platinum(II) centers.

Acidity and Complex Formation

The similarities and differences between the three diaqua complexes were first studied by determining the pK_a values of the coordinated water moieties via spectrophotometric titration with NaOH in the pH range 1–10. A typical example of the spectral changes observed during the pH titration is shown in Fig. 1.

$$\begin{aligned}&[H_2O \cdot Pt(NH_3)_2 \cdot azn \cdot Pt(NH_3)_2 \cdot OH_2]^{4+} \overset{K_{a1}}{\rightleftarrows} \\ &\quad [H_2O \cdot Pt(NH_3)_2 \cdot azn \cdot Pt(NH_3)_2 \cdot \mathbf{OH}]^{3+} + H^+ \\ &[H_2O \cdot Pt(NH_3)_2 \cdot azn \cdot Pt(NH_3)_2 \cdot \mathbf{OH}]^{3+} \overset{K_{a2}}{\rightleftarrows} \\ &\quad [\mathbf{HO} \cdot Pt(NH_3)_2 \cdot azn \cdot Pt(NH_3)_2 \cdot OH]^{2+} + H^+\end{aligned} \tag{2}$$

The spectral data were analyzed as a plot of absorbance against pH (see Fig. 1, inset) and using a nonlinear least-squares fit, gave an excellent fit for a system comprising two dissociation steps (see Eq. (2)) with the equilibrium constants, K_{a1} and K_{a2}, the pK_a values of which are listed in Table I.

Kinetic Measurements

The ligand substitution of the diaqua complexes by a series of neutral nucleophiles, viz. TU, DMTU, and

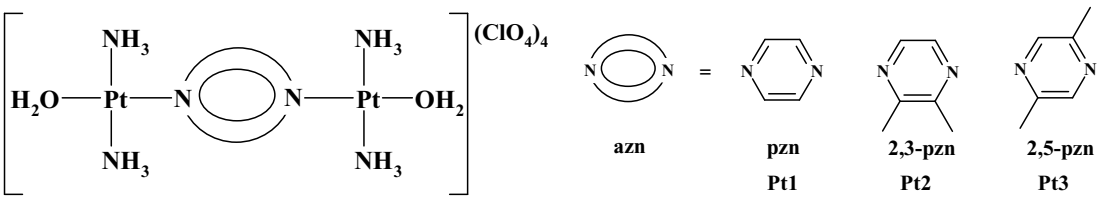

Scheme 1 Structural formulae of the investigated complexes.

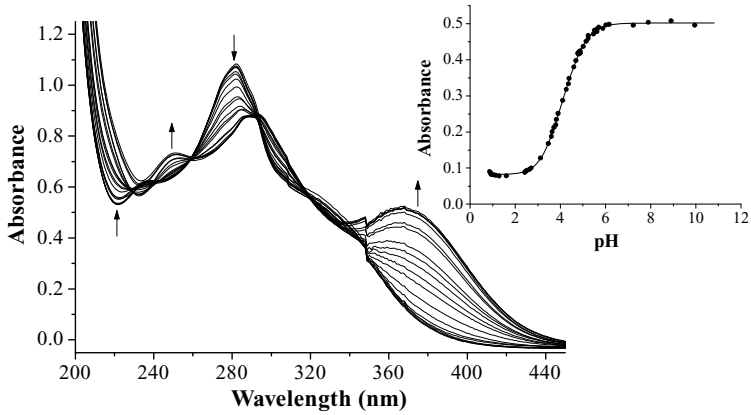

Figure 1 UV–visible spectra recorded for **Pt1** as a function of pH in the range 1–10 at 25.0°C. Inset: Plot of absorbance versus pH at 375 nm.

TMTU, was investigated as a function of concentration and temperature.

The kinetic traces (Fig. 2a) for the ligand substitutions gave excellent fits to a two-exponential function for a system comprising two distinct substitution steps (see Eq. (3)).

$$[H_2O \cdot Pt(NH_3)_2 \cdot azn \cdot Pt(NH_3)_2 \cdot OH_2]^{4+} + Nu \underset{\longleftarrow}{\overset{k_1}{\longrightarrow}} [H_2O \cdot Pt(NH_3)_2 \cdot azn \cdot Pt(NH_3)_2 \cdot \mathbf{Nu}]^{4+} + H_2O$$

$$[H_2O \cdot Pt(NH_3)_2 \cdot azn \cdot Pt(NH_3)_2 \cdot \mathbf{Nu}]^{4+} + Nu \underset{\longleftarrow}{\overset{k_2}{\longrightarrow}} [\mathbf{Nu} \cdot Pt(NH_3)_2 \cdot azn \cdot Pt(NH_3)_2 \cdot \mathbf{Nu}]^{4+} + H_2O \quad (3)$$

The observed rate constants, k_{obs1} and k_{obs2}, obtained for the substitution of the first and second aqua moieties, respectively, were then plotted against the nucleophile concentration (see Fig. 2b).

Table I Summary of pK_a Values for the First and Second Deprotonation Steps of the Diaqua Complexes

Complex Azn Linker	λ(nm)	pK_{a1}	pK_{a2}	ΔpK_a
Pt1	375	3.59 ± 0.33	4.36 ± 0.30	0.77
				
Pt2	365	3.66 ± 0.11	4.61 ± 0.22	0.95
				
Pt3	365	3.68 ± 0.26	4.62 ± 0.21	0.94
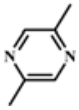				

Representative plots (Fig. 3) for each of the investigated nucleophiles show a linear dependence on the concentration of the incoming nucleophile. The absence of a meaningful intercept indicates that the reverse reaction with water was either negligible or absent thus suggesting that the mechanism of substitution can be given by Eq. (3).

The rate constants, k_1 and k_2, were obtained from the slopes of these plots at 25°C and are summarized in Table II.

The temperature dependence of $k_1$and k_2 was studied over the range 15–35°C. A typical plot is shown in Fig. 4. The activation parameters, $\Delta H^{\neq}$ and $\Delta S^{\neq}$, were calculated using the Eyring equation [59] and are presented in Table II.

DFT Calculations

In an effort to gain further insight into how the bridging azine ligand influences the reactivity of the platinum(II) centers, it was also necessary to assess the molecular structures and electronic properties of the investigated diaqua complexes.

Minimum energy structures (full geometry optimizations) were calculated for each of the diaqua complexes (**Pt1**–**Pt3**) at the B3LYP/LACVP** level of theory. The calculated geometries are acceptable considering the degree of similarity between X-ray and DFT-calculated structures of the corresponding cis analogue, $[\{cis\text{-}Pt(NH_3)_2Cl\}_2(\mu\text{-pzn})]^{2+}$ described by Reedijk et al. [33]. The calculated and observed bond distances were in good agreement. For $[\{cis\text{-}Pt(NH_3)_2Cl\}_2(\mu\text{-pzn})]^{2+}$, the relevant bond distances were (calcd, observed): Pt_a–N_1 (2.067, 2.007 Å), Pt_a–Cl_1(2.332, 2.295 Å), and Pt_a–N_4 (2.147, 2.032 Å).¶

¶See ESI for numbering scheme employed when discussing agreement between calculated and observed bond lengths.

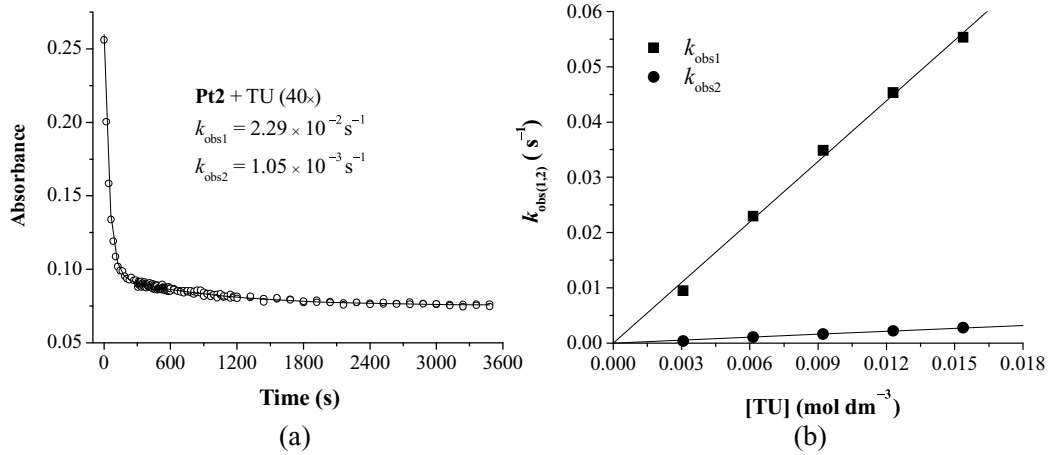

Figure 2 (a) Kinetic trace and two-exponential fit for the reaction of **Pt2** (0.154 mM) and thiourea (TU, 6.15 mM) followed at 340 nm. (b) Plot of observed rate constants, k_{obs1} and k_{obs2}, for the first and second aqua substitutions, respectively, for the reaction between **Pt2** (0.154 mM) and thiourea (TU, 6.15 mM).

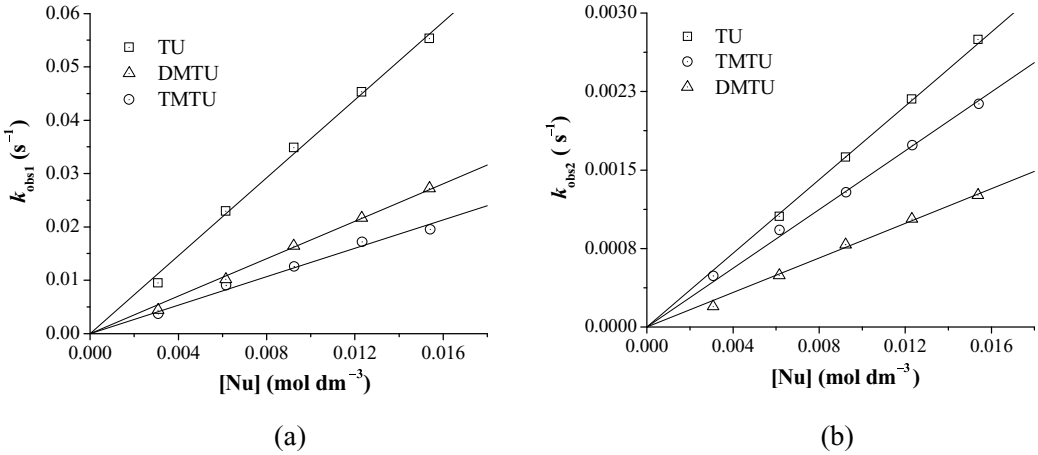

Figure 3 (a) Dependence of the observed rate constants for first aqua substitution (k_{obs1}) from **Pt2** on the entering nucleophile concentration. (b) Dependence of the observed rate constants for second aqua substitution (k_{obs2}) from **Pt2** on the entering nucleophile concentration. Reaction conditions: $I = 0.1$ M (ClO_4^-), pH 2, $T = 298.15$ K.

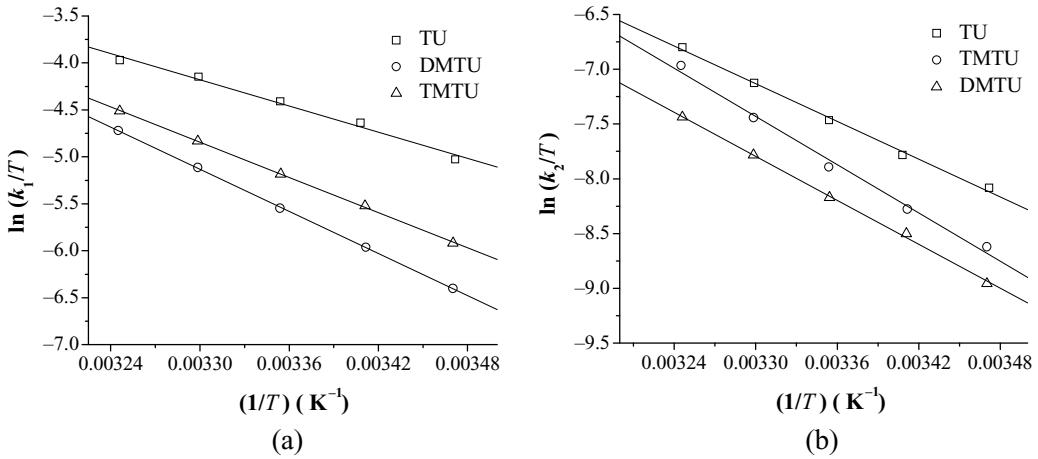

Figure 4 Eyring plots for the determination of the activation parameters, $\Delta H^{\#}_{(1,2)}$ and $\Delta S^{\#}_{(1,2)}$, for the first (a) and second (b) substitution steps for the reaction of **Pt3** (0.138 mM) with the incoming nucleophiles. Reaction conditions: $I = 0.1$ M (ClO_4^-), pH 2.

Table II Summary of Rate Constants and Activation Parameters, with the Corresponding Standard Deviations[a], for the First and Second Aqua Substitutions by a Series of Neutral Nucleophiles. Reaction Conditions: I = 0.1 M (ClO_4^-), pH 2

Complex Azn Linker	Nu	k_1(M^{-1} s^{-1})	k_2(M^{-1} s^{-1})	k_1/k_2	$\Delta H_1^{\#}$(kJ mol^{-1})	$\Delta H_2^{\#}$(kJ mol^{-1})	$\Delta S_1^{\#}$(J K^{-1} mol^{-1})	$\Delta S_2^{\#}$(J K^{-1} mol^{-1})
Pt1	TU	18.43 ± 0.19	1.65 ± 0.03	11.2	43.3 ± 1.1	40.3 ± 3.4	−76.1 ± 3.6	−106.5 ± 11.5
	DMTU	7.86 ± 0.32	0.66 ± 0.10	11.9	43.5 ± 6.9	43.7 ± 3.4	−123.6 ± 23.1	−143.6 ± 11.3
	TMTU	3.83 ± 0.22	0.84 ± 0.08	4.6	32.8 ± 0.3	50.8 ± 6.5	−160.5 ± 1.0	−113.7 ± 21.6
Pt2	TU	3.64 ± 0.05	0.170 ± 0.003	21.4	42.8 ± 1.3	55.2 ± 0.9	−93.5 ± 4.3	−74.8 ± 3.2
	DMTU	1.75 ± 0.03	0.082 ± 0.002	21.3	50.6 ± 1.4	57.2 ± 1.0	−70.8 ± 4.7	−74.0 ± 3.5
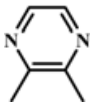	TMTU	1.33 ± 0.03	0.140 ± 0.002	9.5	61.5 ± 3.1	60.8 ± 1.4	−36.8 ± 10	−57.5 ± 4.6
Pt3	TU	3.51 ± 0.04	0.160 ± 0.002	21.9	39.0 ± 2.3	48.3 ± 2.1	−104.0 ± 7.7	−97.8 ± 7.0
	DMTU	1.73 ± 0.03	0.085 ± 0.001	20.4	51.8 ± 0.7	55.7 ± 1.4	−67.2 ± 2.1	−78.8 ± 4.7
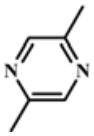	TMTU	1.14 ± 0.03	0.112 ± 0.003	10.2	62.1 ± 0.4	61.1 ± 3.0	−35.7 ± 1.2	−58.2 ± 10.2

[a]Standard deviations obtained for k_2 are those of the slope of the plot of k_{obs} versus nucleophile concentration. Standard deviations for activation parameters obtained are those from the slope ($\Delta H^{\neq}$) and y-intercept ($\Delta S^{\neq}$) obtained from a plot of $\ln(k_2/T)$ versus $1/T$.

Table III Summary of Structural and Electronic Data Obtained from DFT Calculations of Investigated Complexes at the B3LYP/LACVP** Level of Theory

	Pt1	**Pt2**	**Pt3**
Average bond distances (Å)			
$Pt_a/_b$–OH_2	2.100	2.110	2.112
$Pt_a/_b$–*trans* N	2.072	2.085	2.074
Pt_a–Pt_b	6.952	6.950	6.937
MO energies (eV)			
E_{HOMO}	−20.13	−19.80	−19.81
E_{LUMO}	−16.27	−15.54	−15.65
ΔE	3.86	4.26	4.16
Average NBO charges			
Pt_a/Pt_b	1.2438	1.2342	1.2342
O–H_2	−1.0086	−1.0069	−1.0089

Table III summarizes the calculated bond distances, energies of the frontier molecular orbitals, and electron densities surrounding the Pt(II) centers for each of the investigated derivatives. The DFT optimized structures, including their ground state orbitals, are shown in Table IV.

DISCUSSION

In the current study, three azine-bridged dinuclear platinum(II) complexes, viz. [{*trans*-Pt(OH_2)(NH_3)$_2$}$_2$(μ-pzn)](ClO_4)$_4$ (**Pt1**), [{*trans*-Pt(OH_2)(NH_3)$_2$}$_2$(μ-2,3pzn)](ClO_4)$_4$ (**Pt2**), and [{*trans*-Pt(OH_2)(NH_3)$_2$}$_2$(μ-2,5pzn)](ClO_4)$_4$(**Pt3**), were prepared and their kinetic and thermodynamic parameters determined in an effort to rationalize the influence of the bridging azine ligand on the reactivity of the metal centers.

pK_a Determination

The pK_a values obtained for the three diaqua complexes are similar to those obtained previously for similar complexes [42,44].

Previous studies have shown that the pK_a value obtained for the coordinated water moiety at the platinum(II) center is a good indicator of the electrophilicity of the metal center [42,44,60,61]. Electron-withdrawing π-acceptor effects tends to stabilize the electron-rich hydroxo species in comparison to the aqua species and results in lower pK_a values [44,60,61]. Alternatively, if the σ-donor capacity of the ligand trans to the aqua moiety is enhanced, then a higher pK_a value is obtained [62].

For the complexes studied, the addition of methyl groups to the bridging azine ligand in **Pt2** and **Pt3** does indeed result in an increase in the σ-donor capacity of the ligand trans to the aqua moiety and this is reflected by a moderate increase in the pK_a values for

Table IV DFT-Calculated (B3LYP/LACVP**) Molecular Structures and Orbitals, i.e., HOMOs and LUMOs, for the Investigated Diaqua Complexes [Color figure can be viewed in the online issue, which is available at wileyonlinelibrary.com.]

	Pt1	Pt2	Pt3
Geometry Optimized Structure	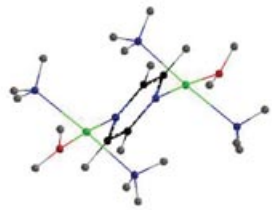		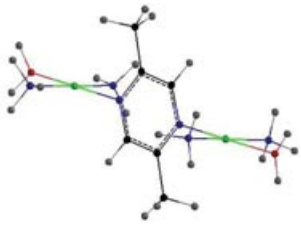
HOMO	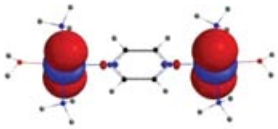	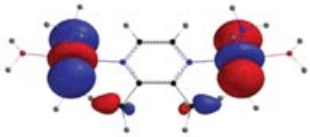	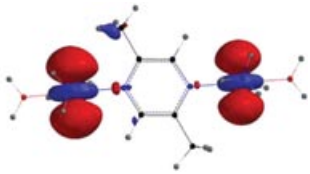
LUMO	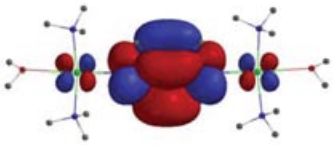	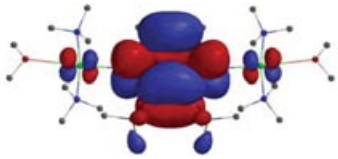	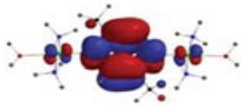

both the first and second deprotonation steps for these complexes, the pK_a values for **Pt2** being 0.07 and 0.25 units greater than that for **Pt1** for the first and second deprotonation steps, respectively.

The pK_a values obtained in the current study compare favorably with that obtained by Hofmann and van Eldik [44]. In comparing the pK_a values of the complexes $[Pt_2(N, N, N', N'$-tetrakis(2-pyridylmethyl)benzene-1, 3-diamine)$Cl_2](ClO_4)_2$ (**mPh**) and $[Pt_2(N, N, N', N'$-tetrakis(2-pyridylmethyl)benzene-1,4-diamine)$Cl_2](ClO_4)_2$ (**pPh**), the authors found values of 3.33/4.76 and 3.34/4.46 for the two deprotonation steps, respectively, which are remarkably similar to those obtained in the current study.

We also observe that the difference in pK_a values ($\Delta pK_a = pK_{a2} - pK_{a1}$) increases upon the addition of methyl groups to the bridging ligand from 0.8 for **Pt1** to 0.9 for **Pt2** and **Pt3**, with the value of the second deprotonation step is ca. 1.2 times that of the first.

This effect has been observed previously by Hofmann and van Eldik [44]. In comparing the pK_a values of the complexes **mPh** and **pPh**, they found that the ΔpK_a for **mPh** is 1.43 compared to a value of 1.12 for **pPh**. The authors explained the effect as being due to the average distance between the two platinum centers, which impact on the interaction between the metal centers and subsequently their pK_a values. In this instance, the ΔpK_a value for **pPh** is lower than that of **mPh** as a result of a longer Pt–Pt distance.

In the current study, the average Pt–Pt distance for **Pt1** and **Pt2** are similar but are slightly longer than that for **Pt3** (see Table III). On the basis of the explanation by Hofmann and van Eldik [44], one would expect the pK_a for **Pt1** and **Pt2** to be the same if only the distance between the platinum centers was the controlling factor. From the pK_a data obtained (Table I), we find that this is not true, with all pK_a values being equivalent if statistical differences are taken into account. The other expectation was that the introduction of the methyl substituents on the pyrazine moiety would result in an increased electronic effect that would result in the Pt–OH_2bond being longer and, consequently, the pK_a values of the respective complex would be higher. This is indeed true, as the results show that the pK_a values obtained for **Pt2** and **Pt3** are higher than that of **Pt1** due to the inductive effect. It can therefore be suggested that the introduction of the methyl groups to the pyrazine linker reduces, through the inductive effect, the positive charge on the metal center. This suggestion is further supported by the DFT-calculated average NBO charges, as indicated in Table III. The net effect of this is higher pK_a values for **Pt2** and **Pt3**.

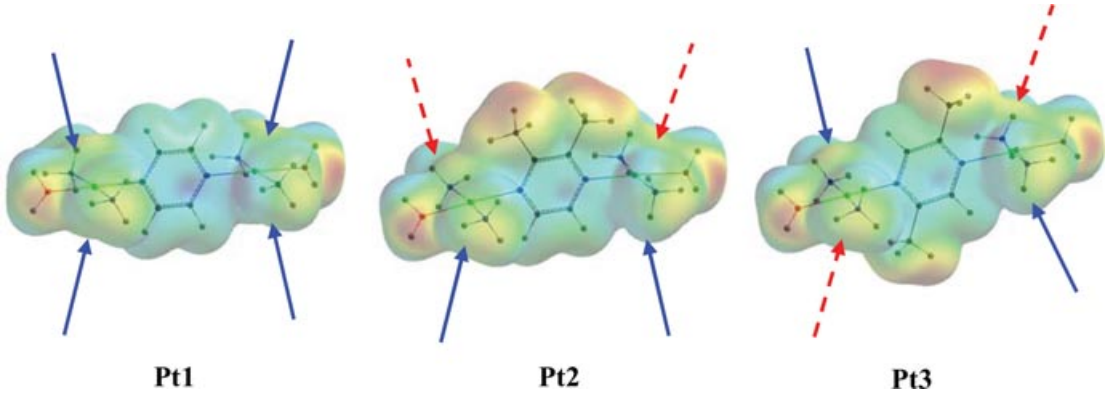

Figure 5 DFT-calculated electron-density distribution plots for the investigated diaqua complexes illustrating the steric hindrance imposed by the bridging azine ligand for **Pt2** and **Pt3**. The solid (blue) arrows indicate the least sterically hindered pathways for the incoming nucleophile, whereas the dashed (red) arrows indicated pathways that are subject to increased steric hindrance by the methyl groups present on the bridging azine ligand. [Color figure can be viewed in the online issue, which is available at wileyonlinelibrary.com.]

Ligand Substitutions

On the basis of the results obtained from the pK_a determination, in that the lower pK_a value the greater the electrophilicity of the metal center [42,44,61,62], a fact that is supported by the DFT calculation of the NBO charges as presented in Table III, one would expect that substitution of the aqua moieties by thiourea and its substituted derivatives would follow very much a similar trend in that the rate of ligand substitution would decrease in the case of **Pt2** and **Pt3** as a result of the increased σ-inductive effect due to the additional methyl groups on the bridging azine ligand.

Indeed, the reactivity of **Pt1** is much greater than either **Pt2** or **Pt3**, with the k_1 value for **Pt1** being ca. five times greater than that for either **Pt2** or **Pt3** and that the k_2 value is nearly 10 times greater than that obtained for **Pt2** or **Pt3**, in the case of substitution by TU.

This observation can be attributed to two factors that must be simultaneously playing a role in controlling the substitution process. The first one is the increase in the σ-inductive effect, as explained above. The second is the increased steric hindrance imparted by the methyl groups present on the bridging ligand for both **Pt2** and **Pt3**. The methyl groups restrict the path of the incoming nucleophile to one side of the square plane of the platinum(II) centers. This is readily seen from a plot of the electron-density distribution about the complex (Fig. 5), which clearly shows how the introduction of the methyl groups to the bridging ligand effectively reduces the availability of the metal center to attack by the incoming nucleophile. The percentage reduction is the same for both **Pt2** and **Pt3**, even though the phases through which the reduction takes place are different.

This correlates nicely with previous work with the *cis* derivatives of these complexes, viz. $[\{cis\text{-}PtCl(NH_3)_2\}_2\text{-}\mu\text{-pzn}]^{2+}$ (i) and $[\{cis\text{-}PtCl(NH_3)_2\}_2\text{-}\mu\text{-}2,5\text{-pzn}]^{2+}$ [33,34] (ii), where substitution of the chloride moieties by 9-ethylguanine (9-EtG) from **(i)** proceeds faster than from (ii). The authors attributed this to the steric retardation imposed by the methyl groups present on the bridging ligand in (ii).

In addition, the introduction of the methyl groups to the bridging azine ligands leads to an increase in the energy separation of the frontier molecular orbitals (see Table III; $\Delta E = E_{HOMO} - E_{LUMO}$) of the ground state platinum(II) complexes. This in turn leads to a less reactive metal center, as been observed previously [63].

Also observed is the fact that increasing the steric nature of the incoming nucleophile results in a corresponding decrease in the k values obtained for the investigated complexes with one exception. The k_2 values obtained for substitution of the second aqua moiety from all complexes show that the more sterically bulky TMTU reacts at least 1.3 times faster than DMTU in all the complexes investigated.

A similar effect was noted previously for the substitution of water from $[Pt(bmpa)(OH_2)]^{2+}$ by DMTU and TU, with DMTU reacting faster than TU [64]. In this instance, the authors attributed the effect to the greater inductive effect for DMTU over TU, which overcame steric hindrance, and indeed the case may be that the inductive effect of TMTU is greater than that of DMTU and that via some form of "trans-effect" through the azine linker, leads to a moderate increase in the rate of substitution of the second aqua moiety.

This is supported by DFT calculations of the monosubstituted complexes (Table V), which show clearly that following substitution of the first aqua moiety, there is subsequently moderate bond lengthening of the Pt–OH_2 bond and bond shortening of the Pt–*trans* N bond.

Table V Summary of Structural Data Obtained from DFT Calculations of the Unsubstituted and Monosubstituted Complexes at the B3LYP/LACVP** Level of Theory

	Pt1	Pt2	Pt3
Pt—OH_2 (Å)			
Pt_a—OH_2	2.099	2.110	2.111
Pt_b—OH_2	2.100	2.110	2.112
Pt_b—OH_2 (+TU)	2.108	2.119	2.117
Pt_b—OH_2 (+DMTU)	2.110	2.118	2.119
Pt_b—OH_2 (+TMTU)	2.112	2.121	2.121
Pt–*trans* N (Å)			
Pt_a—N3	2.071	2.084	2.072
Pt_b—N4	2.072	2.085	2.076
Pt_b—N4 (+TU)	2.063	2.073	2.068
Pt_b—N4 (+DMTU)	2.060	2.072	2.064
Pt_b—N4 (+TMTU)	2.058	2.070	2.063
Dihedral angle (°)			
C1–N3–Pt_a—N1/C2–N4–Pt_b–N5	90.35	93.17	89.49
C2–N4–Pt_b—N5 (+TU)	91.64 (+1.29)	92.68 (−0.49)	88.72 (−0.77)
C2–N4–Pt_b—N5 (+DMTU)	90.69 (+0.34)	92.35 (−0.82)	87.17 (−2.32)
C2–N4–Pt_b—N5 (+TMTU)	91.08 (+0.73)	93.08 (−0.09)	90.89 (+1.40)

For labeling scheme employed, see Fig. 6.

Pt_a represents the substituted metal center and Pt_b the unsubstituted metal center, before and after substitution at Pt_a, respectively.

Values in parentheses for the dihedral angles of the monosubstituted complexes show the deviation from that for the diaqua (unsubstituted) complex.

However, the question that must then be asked is why substitution of the second aqua moiety by DMTU is not faster than that by TU. Does this "effect" become noticeable only for the larger nucleophiles, or is TMTU substituting the second aqua moiety slightly faster than DMTU as a result of a combination of effects?

Looking at the structures of the diaqua complexes (Table IV, Fig. 6), we see also that the square plane of the metal center is almost perpendicular to that of the bridging azine ligand (Fig. 6b). This is not unexpected, as X-ray structures of other metal complexes containing similar aromatic bridging ligands also show the aromatic linker being almost perpendicular to the plane of the complex [65,66].

We find that upon substitution of the first aqua moiety from the first platinum center, this plane is slightly offset.

We find that the amount by which this dihedral angle, C2–N4–Pt_b–N5 (from Fig. 6), deviates from 90° relates to the relative ease with which the incoming nucleophile might approach the second metal center. This provides an explanation as to why substitution of the second aqua moiety by TMTU occurs slightly faster than that by DMTU, in that despite the increased steric bulk of the nucleophile, its approach to the second metal center is not as sterically hindered as that for DMTU. It also provides an explanation as to why the k_2 value for **Pt2** is slightly bigger than that of **Pt3**.

Overall, the rate of substitution of the first aqua moiety, k_1, is greater than that of the second, k_2 (see Table II), with substitution by both TU and DMTU resulting in k_1 values ca. 20 times greater than k_2 values in the case of both **Pt2** and **Pt3**. In the case of substitution by TMTU, this ratio is reduced by almost half. Again, a combination of the "trans-effect" through the azine linker and deviation of the dihedral angle appears to ease the rate of ligand substitution by TMTU at the second platinum center.

Activation parameters obtained for substitution of both aqua moieties support an associative mode of activation with the activation enthalpies being relatively low and activation entropies all large and negative. We find that the activation enthalpies obtained for both **Pt2** and **Pt3** are slightly larger than that for **Pt1**, again reflecting the influence of the additional methyl groups on the bridging azine ligand on the reactivity of the metal centers.

The activation enthalpies obtained for the first and second substitutions at **Pt1**, $\Delta H_1^{\#}$ and $\Delta H_2^{\#}$, are of the same order for both TU and DMTU as the incoming nucleophile, suggesting that the unsubstituted bridging ligand does not hinder the path of the incoming nucleophile. This is also reflected in the activation entropies, $\Delta S_1^{\#}$ and $\Delta S_2^{\#}$, which are of similar orders.

The activation enthalpy for the first TMTU substitution is relatively low, whereas that for the second TMTU substitution it is ca. 18 kJ mol^{-1} higher,

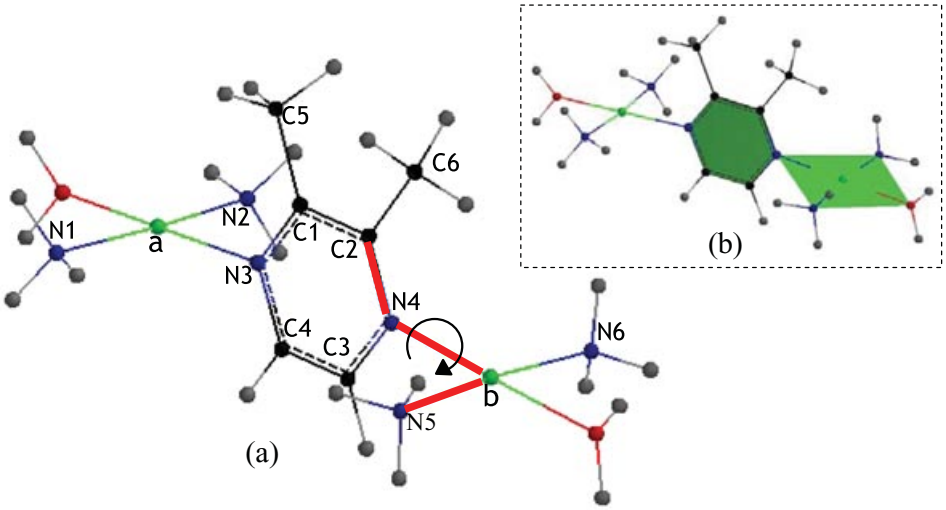

Figure 6 (a) Structure of **Pt2** shown with labeling scheme employed. Rotation about the N4-Pt_b bond; see the dihedral, C2–N4–Pt_b–N5, twisting slightly away from the perpendicular so as to accommodate the incoming nucleophile at the second substitution site, with the deviation being greater when TMTU is the incoming nucleophile than when DMTU is. (b) The metal square plane lying almost perpendicular to the plane of the bridging ligand. [Color figure can be viewed in the online issue, which is available at wileyonlinelibrary.com.]

indicating that the first-bound TMTU hinders the path of the incoming TMTU at the second substitution site. Again, this is supported by the activation entropy for the second substitution, $\Delta S_2^{\#}$, which is slightly more positive than that for the first substitution step.

The activation enthalpies obtained for the first and second substitution steps by TU and DMTU at **Pt2** and **Pt3** show slight increases for the second substitution step due to the greater steric hindrance imposed by the methyl groups on the bridging azine ligand *and* the first-bound nucleophile on the path of the second-incoming nucleophile. The activation entropies obtained for the second substitution are slightly more positive than those obtained for **Pt1**, thus supporting the conclusion drawn above.

The activation enthalpies obtained for the first and second substitutions by TMTU in both **Pt2** and **Pt3** are ca. the same at 60 J K^{-1} mol^{-1}. This can be attributed to the slight twisting at the dihedral angle, C2–N4–Pt_b–N5, described earlier, which allows the incoming TMTU to approach the second substitution site with less steric constraint. This is reflected by the $\Delta S_2^{\#}$ value, which is more negative for the second TMTU substitution than for the first TMTU substitution, $\Delta S_1^{\#}$.

CONCLUSIONS

The results presented in this paper clearly show the dependence of the reactivity of the metal center on the nature of the rigid bridging azine ligand trans to the leaving group. The pK_a values obtained clearly show that increasing the σ-donor capacity of the bridging ligand trans to the aqua moiety leads to a higher pK_a value, which reflects the reduced electrophilicity of the metal center and leads to a less-reactive metal center.

This is mirrored by the rate constants obtained for the substitution of the aqua moiety by thiourea and its substituted derivatives. The k-values obtained for **Pt1** are much greater than either **Pt2** or **Pt3**, which shows that introduction of the methyl groups to the bridging azine ligand does indeed lead to a less-reactive metal center. This results from a combination of steric and electronic effects.

From DFT calculations, we find that the bridging azine ligand lies almost perpendicular to the square plane of the metal center and thus the methyl groups on the bridging ligands effectively "shadow" the metal center effectively, reducing the path of approach for the incoming nucleophile. In addition to this steric effect, the introduction of the methyl groups to the bridging azine ligand leads to an increase in the energy separation of the frontier molecular orbitals (ΔE) that leads to a less-reactive metal center in the ground state.

The slight differences between the k_2 values obtained for substitution by DMTU and TMTU, respectively, can be explained by the slight structural differences that occur upon substitution of the first aqua moiety, which allows for slightly easier approach when the incoming nucleophile is TMTU.

This is reflected by the activation enthalpies and entropies, which for both **Pt2** and **Pt3**, show that the

$\Delta H^{\#}_{1,2}$ values are of approximately the same order and the $\Delta S^{\#}_2$ value being more negative than the $\Delta S^{\#}_1$ value when the incoming nucleophile is TMTU. The mode of activation remains associative in nature.

Thus, the study clearly shows that the nature of the bridging azine ligand does influence the reactivity at both the metal centers due to its σ-donor capacity and steric influence, which result in ground-state destabilization of the dinuclear platinum(II) complex.

SUPPORTING INFORMATION

Supporting Information includes a summary of selected wavelengths used in the kinetic investigations, measured rate constants and representative plots pertaining to this study and is available in the online issue at www.wileyonlinelibrary.com.

DR acknowledges financial support from the Carl and Emily Fuchs Foundation.

BIBLIOGRAPHY

1. Rosenberg, B.; Van Camp, L.; Krigas, T. Nature 1965, 205, 698.
2. Rosenberg, B.; Van Camp, L.; Trosko, J. E.; Mansour, V. H. Nature 1969, **222**, 385.
3. Ash, D. C. J Clin Hemat Oncol 1980, 10, 55.
4. Chu, G. J Biol Chem 1994, 269, 787.
5. Lippert, B. (Ed.). Cisplatin. Chemistry and Biochemistry of a Leading Anticancer Drug; Wiley-VCH: New York, 1999.
6. Wong, E.; Giandomenico, C. M. Chem Rev 1999, 99, 2451.
7. Jaimeson, E. R.; Lippard, S. J. Chem Rev 1999, 99, 2467.
8. Giacocone, G. Drugs 2000, 59, 9.
9. Schaefer, S. D.; Post, J. D.; Close, L. G.; Wright C. G. Cancer 1985, 56, 1934.
10. Goren, M. P.; Wright, R. K.; Horowitz, M. E. Cancer Chemother Pharmacol 1986, 18, 69.
11. Alberts, D. S.; Noel, J. K. Anticancer Drugs 1995, 6, 369.
12. Perez, R. P.; Hamilton, T. C.; Ozols, R. F.; Young, R. C. Cancer 1993, 71, 1571.
13. Cleare, M. J.; Hoeschele, J. D. Plat Met Rev 1973, 17, 3.
14. Cleare, M. J.; Hoeschele, J. D. Bioinorg Chem 1973, 2, 187.
15. Farrell, N. P.; de Almeida, S. G.; Skov, K. A. J Am Chem Soc 1988, 110, 5018.
16. Farrell, N.; Qu, Y. Inorg Chem 1989, 28, 3416.
17. Farrell, N., Qu, Y.; Hacker, M. P. J Med Chem 1990, 33, 2179.
18. Komeda, S.; Lutz, M.; Spek, A. L.; Chikuma, M.; Reedijk, J. Inorg Chem 2000, 39, 4230.
19. Wheate, N. J. Cullinane, C. Webster, L. K.; Collins, J. G. Anti-Cancer Drug Design 2001, 16, 91.
20. Jansen, B. A. J.; Van Der Zwan, J.; den Dulk, H.; Brouwer, J; Reedijk, J. J Med Chem 2001, 44, 245.
21. Komeda, S; Lutz, M.; Spek, A. L.; Yamanaka, Y.; Sato, T.; Chikuma, M.; Reedijk, J. J Am Chem Soc 2002, 124, 4738.
22. Kas'yanenko, N. A.; Aia, E. E. F.; Bogdanov, A. A.; Kosmotynskaya, Y. V.; Yakovlev, K. I. Mol Biol 2002, 36, 745.
23. Wheate, N. J.; Collins, J. G. Coord Chem Rev 2003, 241, 133.
24. Ho, Y-P.; Au-Yeung, S. C. F.; To, K. K. W. Med Res Rev 2003, 23, 633.
25. Wheate, N. J.; Collins, J. G. Curr Med Chem Anti-Cancer Agents 2005, 5, 267.
26. McGregor, T. D.; Balcarova, Z.; Qu, Y.; Tran, M.-C.; Zaludova, R.; Brabec, V.; Farrell, N. J Inorg Biochem 1999, 77, 43.
27. Kasparkova, J.; Vrana, O.; Farrell, N.; Brabec, V. J Inorg Biochem 2004, 98, 1560.
28. Fichtinger-Schepman, A. M. J.; Van der Veer, J. L.; Den Hartog, J. H. J.; Lohman, P. H. M.; Reedijk, J. Biochemistry 1985, 24, 707.
29. Yang, S. V. D. Z.; Reedijk, J.; Vanboom, J. H.; Farrell, N.; Wang, A. H. J. Nat Struct Biol 1995, 2, 577.
30. Eastman, A; Schulte, N. Biochemistry 1988, 27, 4730.
31. Liu, Q.; Qu, Y.; van Antwerpen, R.; Farrell, N. Biochemistry 2006, 45, 4248.
32. Rauter, H.; Di Domenico, R.; Menta, E.; Oliva, A.; Qu, Y.; Farrell, N. Inorg Chem 1997, 36, 3919.
33. Komeda, S.; Kalayda, G. V.; Lutz, M.; Spek, A. L.; Yamanaka, Y.; Sato, T.; Chikuma, M.; Reedijk, J. J Med Chem 2003, 46, 1210.
34. Kalayda, G. V.; Komeda, S.; Ikeda, K.; Sato, T.; Chikuma, M.; Reedijk, J. Eur J Inorg Chem 2003, 4347.
35. Kalayda, G. V.; Jansen, B. A. J.; Wielard, P.; Tanke, H. J.; Reedijk, J. J Biol Inorg Chem 2005, 10, 305.
36. Farrell, N.; Appleton, T. G.; Qu, Y.; Roberts, J. D.; Fontes, A. P. S.; Skov, K. A.; Wu, P.; Zou, Y.; Biochemistry 1995, 34, 15480.
37. Brabec, V.; Kasparkova, J.; Vrana, O.; Novakova, O.; Cox, J. W.; Qu, Y.; Farrell, N.; Biochemistry 1999, 38, 6781.
38. Davies, M. S.; Cox, J. W.; Berners-Price, S. J.; Barklage, W.; Qu, Y.; Farrell, N. Inorg Chem 2000, 39, 1710.
39. Davies, M. S.; Thomas, D. S.; Hegmans, A.; Berners-Price, S. J.; Farrell, N. Inorg Chem 2002, 41, 1101.
40. Komeda, S.; Yamane, H.; Chikume, M.; Reedijk, J. Eur J Inorg Chem 2004, 4828.
41. Jaganyi, D.; Munisamy, V. M.; Reddy, D. Int J Chem Kinet 2006, 38, 202.
42. Ertürk, H.; Hofmann, A.; Puchta, R.; van Eldik, R. Dalton Trans 2007, 2295.

43. Summa, N.; Maigut, J.; Puchta, R.; van Eldik, R. Inorg Chem 2007, 46, 2094.
44. Hofmann A.; van Eldik, R. Dalton Trans 2003, 2979.
45. Ertürk, H.; Maigut, J.; Puchta, R.; van Eldik, R. Dalton Trans 2008, 2759.
46. Lippert, B.; Pfab, R.; Neugebauer, D. Inorg Chim Acta 1979, 37, L495.
47. Hollis, L. S.; Amundsen, A. R.; Stern, E. W. J Med Chem 1989, 32, 128.
48. Bugarćić, Z. D.; Petrović, B. V.; Jelić, R. Transition Met Chem 2001, 26, 668.
49. Spartan '04, Wavefunction, Inc., Irvine, CA; Q-Chem, Inc., Pittsburgh, PA, 2004. http://www.wavefun.com/
50. Kong, J.; White, C. A.; Krylov, A. I.; Sherrill, C. D.; Adamson, R. D.; Furlani, T. R.; Lee, M. S.; Lee, A. M.; Gwaltney, S. R.; Adams, T. R.; Ochsenfeld, C., B.; Gilbert, A. T.; Kedziora, G. S.; Rassolov, V. A.; Maurice, D. R.; Nair, N.; Shao, Y.; Besley, N. A.; Maslen, P. E.; Dombroski, J. P.; Daschel, H.; Zhang, W.; Korambath, P. P.; Baker, J.; Byrd, E. F. C.; Van Voorhuis, T.; Oumi, M.; Hirata, S.; Hsu, C.-P.; Ishikawa, N.; Florian, J.; Warshel, A.; Johnson, B. G.; Gill, P. M. W.; Head-Gordon, M.; Pople, J. A. J Comput Chem 2000, 21, 1532.
51. Becke, A. D. J Chem Phys 1993, 98, 5648.
52. Friesner, R. A. Chem Phys Lett 1985, 116, 39.
53. Friesner, R. A. Annual Rev Phys Chem 1991, 42, 341.
54. Hay, P. J.; Wadt, W. R. J Chem Phys 1985, 82, 299.
55. Rassolov, V. A.; Pople, J. A.; Ratner, M. A.; Windus, T. L. J Chem Phys 1998, 109, 1223.
56. Francl, M. M.; Pietro, W. J.; Hehre, W. J.; Binkley, J. S.; Gordon, M. S.; DeFrees, D. J.; Pople, J. A. J Chem Phys 1982, 77, 3654.
57. Appleton, T. G.; Hall, J. R.; Ralph, S. F.; Thompson, C. S. M. Inorg Chem 1984, 23, 3521.
58. Microcal^{TM} Origin^{TM} Version 7.5, Microcal Software, Inc., Northampton, MA, 1991–2003.
59. Atwood, J. D., Inorganic and Organometallic Reaction Mechanisms, 2nd ed.; Wiley-VCH Inc.: New York, 1997; pp. 43–61.
60. Jaganyi, D.; Hofmann, A.; van Eldik, R. Angew Chem, Int Ed 2001, 40, 1680.
61. Hofmann, A.; Jaganyi, D.; Munro, O. Q.; Liehr, G.; van Eldik, R. Inorg Chem, 2003, 42, 1688.
62. Schmülling, M.; Grove, D. M.; van Koten, G.; van Eldik, R.; Veldman, N.; Spek, A. L. Organometallics 1996, **15**, 1384.
63. Reddy, D.; Jaganyi, D. Dalton Trans 2008, 6724.
64. Jaganyi, D.; Tiba, F.; Munro, O. Q.; Petrović, B.; Bugarćić, Z. D. Dalton Trans 2006, 2943.
65. Schindler, S.; Szalda, D. J.; Creutz, C. Inorg Chem 1992, 31, 2255.
66. Hazell, A.; McKenzie, C. J.; Nielsen, L. P. J Chem Soc, Dalton Trans 1998, 1751.